



HAL
open science

Molten Salt-Shielded Synthesis (MS 3) of MXenes in Air

Jinjin Chen, Qianqian Jin, Youbing Li, Hui Shao, Pengcheng Y Liu, Ying Liu, Pierre-Louis Taberna, Qing Huang, Zifeng Lin, Patrice Simon

► **To cite this version:**

Jinjin Chen, Qianqian Jin, Youbing Li, Hui Shao, Pengcheng Y Liu, et al.. Molten Salt-Shielded Synthesis (MS 3) of MXenes in Air. ENERGY & ENVIRONMENTAL MATERIALS, 2022, 15, 10.1002/eem2.12328 . hal-03826833

HAL Id: hal-03826833

<https://hal.science/hal-03826833v1>

Submitted on 9 Nov 2022




HAL is a multi-disciplinary open access archive for the deposit and dissemination of scientific research documents, whether they are published or not. The documents may come from teaching and research institutions in France or abroad, or from public or private research centers.

L'archive ouverte pluridisciplinaire **HAL**, est destinée au dépôt et à la diffusion de documents scientifiques de niveau recherche, publiés ou non, émanant des établissements d'enseignement et de recherche français ou étrangers, des laboratoires publics ou privés.



Distributed under a Creative Commons Attribution - NonCommercial - NoDerivatives 4.0 International License

Molten Salt-Shielded Synthesis (MS³) of MXenes in Air

Jinjin Chen, Qianqian Jin, Youbing Li, Hui Shao, Pengcheng Liu, Ying Liu* ,
Pierre-Louis Taberna, Qing Huang, Zifeng Lin* , and Patrice Simon* 

MXenes are two-dimensional transition metal carbides and/or nitrides with unique physiochemical properties and have attracted extensive interest in numerous fields. However, current MXene synthesis methods are limited by hazardous synthesis conditions, high production costs, or difficulty in large-scale production. Therefore, a general, safe, cost-effective, and scalable synthesis method for MXenes is crucial. Here, we report the fast synthesis of MXenes in the open air using a molten salt-shielded synthesis (MS³) method, which uses Lewis-acid salts as etchants and a low-melting-point eutectic salt mixture as the reaction medium and shield to prevent MXene oxidation at high temperatures. Carbide and nitride MXenes, including Ti₃C₂T_x, Ti₂CT_x, Ti₃CNT_x, and Ti₄N₃T_x, were successfully synthesized using the MS³ method. We also present the flexibility of the MS³ method by scaling the etching process to large batches of 20 and 60 g of Ti₃AlC₂ MAX precursor in one pot. When used as negative electrodes, the prepared MS³-MXenes delivered excellent electrochemical properties for high-rate Li-ion storage.

1. Introduction

MXenes, a family of two-dimensional (2D) transition metal carbides and carbonitrides prepared from MAX phase precursors by selective etching of the A-site element, are promising materials for energy

J. Chen, P. Liu, Prof. Y. Liu, Prof. Z. Lin, Prof. P. Simon
College of Materials Science and Engineering, Sichuan University, Chengdu 610065, China

E-mail: liuying5536@scu.edu.cn;

E-mail: linzifeng@scu.edu.cn

Dr. Q. Jin

Materials Science and Engineering Research Center, Guangxi University of Science and Technology, Liuzhou 545006, China

Dr. Y. Li, Prof. Q. Huang

Engineering Laboratory of Advanced Energy Materials, Ningbo Institute of Materials Technology and Engineering, Chinese Academy of Sciences, Ningbo 315201, China

Qianwan Institute of CNiTECH, Zhongchuangyi Road, Hangzhou Bay District, Ningbo 315336, China

Dr. H. Shao, Prof. P. L. Taberna, Prof. P. Simon

CIRIMAT, Université de Toulouse, CNRS, Toulouse 31400, France


Réseau sur le Stockage Electrochimique de l'Energie (RS2E), FR CNRS no 3459

E-mail: simon@chimie.ups-tlse.fr

Prof. Z. Lin

Engineering Research Center of Alternative Energy Materials & Devices, Ministry of Education, China

E-mail: linzifeng@vip.163.com

 The ORCID identification number(s) for the author(s) of this article can be found under <https://doi.org/10.1002/eem2.12328>.

DOI: 10.1002/eem2.12328

storage applications.^[1,2] The general formula of MXenes is M_{n+1}X_nT_x (n = 1, 2, 3, or 4), where M is a transition metal(s), X is carbon and/or nitrogen, and T_x represents the surface terminations (-OH, -O, -F, -Cl, etc.).^[3] MXene synthesis is based on the selective etching of the A-layer of the corresponding MAX phase in F-containing solutions, such as HF or a LiF + HCl mixture.^[4] However, these methods pose significant risks to human safety and the environment owing to the formation of toxic and corrosive HF; thus, HF-free methods for MXene preparation are urgently needed. HF-free methods, such as electrochemical etching,^[5] molten salt etching,^[6] and hydrothermal routes,^[7] have been reported, but they require hours to days to prepare MXenes. In addition, most of the synthesis methods are only effective for etching Al-containing MAX phases, making them unsuitable for MAX phase precursors with other A-site elements (such as Si, Ga, and Zn). In 2020, a Lewis molten salt etching method was proposed for etching MAX phases with various A-site elements, which expands the potential range of MAX phase precursors.^[8] However, because of their oxidation sensitivity, MXenes are chemically unstable,^[9] particularly at high temperatures. Consequently, inert gas protection is required during synthesis that may cause complexity in synthesis procedures and experimental facilities, resulting in increased production costs.

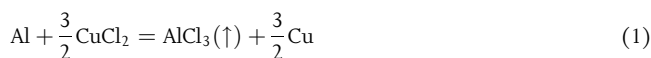
In 2019, a molten salt-shielded synthesis (MS³) method was proposed to prepare various oxidation-sensitive materials, such as porous Ti, Ti₃SiC₂, and Ti₂AlN MAX phases, under an air atmosphere.^[10] In this process, low-melting-point KBr is used as a reaction medium to protect products from oxidation during high-temperature synthesis by forming a protective molten salt layer around the sample at low temperatures. Inspired by the MS³ method of MAX phases synthesis and Lewis salt etching synthesis of MXenes, we recently proposed the preparation of MXenes by a one-pot molten salt synthesis method using M, A, and X (carbon) elements as precursors.^[11] Ti₃C₂T_x and Ti₂CT_x MXenes were obtained by two consecutive steps that occurred in the reactor: in-situ MAX phase synthesis at 1300 °C followed by in situ Lewis salt etching at 700 °C. This one-pot method enables the synthesis of carbide MXenes directly from elemental precursors for the first time, and the entire process was achieved in <8 h without inert gas protection. The one-pot synthesis strategy relies on the in-situ synthesis of MAX phases in molten salts, however, some MAX phases, such as Nb-based, most 413 and 514 MAX phases, have not been achieved by the molten salt method due to the severe volatilization of molten salts at the high synthesis temperatures near or beyond their boiling points,^[12–14]

which hinders the synthesis of corresponding MXenes (such as Nb₂C, Nb₄C₃, etc.) by one-pot synthesis method. Therefore, preparing MXenes by using MAX phases precursors is still indispensable by far.

In this study, the MS³ method was used to prepare MXenes with the corresponding MAX phases as precursors and the CuCl₂ Lewis salt as the etchant. Similarly, low-melting-point eutectic chlorides (NaCl + KCl) were employed as the salt bed to provide a molten salt environment and avoid direct contact between the reactants and the air atmosphere at high temperatures. Several carbide MXenes, as well as nitride MXenes that are typically difficult to be achieved by other methods, were successfully synthesized without inert gas protection in considerably less time. The scalability of the MS³ method was validated by etching large batches of 20 and 60 g of Ti₃AlC₂ MAX phase into the corresponding Ti₃C₂T_x MXene. When used as lithium storage anodes, the prepared MXenes exhibited superior lithium storage performance.

2. Results and Discussion

Figure 1a depicts a schematic of the MS³ process of the Ti₃C₂T_x MXene under an air atmosphere. A NaCl/KCl and Ti₃AlC₂ MAX mixture was first pressed in a steel die to form a pellet and then placed in a crucible with a NaCl/KCl/CuCl₂ mixture covering the surface. The crucible was then heated to 700 °C in a muffle furnace under an air atmosphere. During heating, the NaCl/KCl/CuCl₂ eutectic salts began melting at approximately 300 °C, which is far below the reaction temperature for MXene etching.^[8] Indeed, the molten salt provided a shielding shell that separated the Ti₃AlC₂ MAX phase from the air.^[10] The Al etching reaction began at 700 °C by the reduction of Cu²⁺ from the molten Lewis acid to Cu and the concomitant oxidation of Al in the Ti₃AlC₂ MAX phase to produce the corresponding Ti₃C₂T_x MXene as discussed in our previous work (see Equation 1).^[8] After etching (10–40 min) at around 700 °C, the crucible was removed and cooled to room temperature in air. The samples were then washed with deionized water to remove the solidified salt and with a 0.5 M ammonium persulfate (APS) acid solution to remove the reduced Cu particles produced during etching. The final MS³-MXene samples were obtained after vacuum filtration and drying at 60 °C for 24 h under vacuum. Several other types of MXenes, including Ti₄N₃T_x, Ti₃CNT_x, and Ti₂CT_x, were also prepared following the same procedure.



The X-ray diffraction (XRD) patterns of pristine Ti₃AlC₂ before and after molten salt etching for 10–40 min at 700 °C are shown in Figure 1b. After 20 min of etching, the diffraction peaks of the Ti₃AlC₂ MAX phase disappeared, while sharp diffraction peaks of the Ti₃C₂T_x MXene were observed.^[15] Even after 10 min of etching, the (00l) peaks of the Ti₃C₂T_x MXene remained noticeable. The (002) peak of the etched samples left shifted from 2θ = 9.49° to 7.94°, which corresponds to an increase in the interlayer spacing from 0.93 to 1.11 nm. Figure 1c–f present the scanning electron microscopy (SEM) images of the Ti₃C₂T_x MXenes etched for 10, 20, 30, and 40 min at 700 °C; all MXene particles exhibit the typical expected multilayered structure. Energy-dispersive X-ray spectroscopy (EDS) mapping (Figure S1) confirmed the homogenous distribution of Ti, C, Al, Cl, Cu, and O. The Al-to-Ti ratio decreased from 1:3 to 0.022:3 after 40 min of etching (Table S1), indicating the successful removal of Al from the pristine Ti₃AlC₂ MAX precursor.

Transmission electron microscopy (TEM) images show that the Ti₃C₂T_x MXene (Figure 1g) had a ribbon-like structure containing tens of restacked Ti₃C₂T_x atomic layers, which explains well the sharp XRD peaks. Atomically resolved high-angle annular dark-field scanning transmission electron microscopy (HAADF-STEM) images along the [11 $\bar{2}$ 0] and [1 $\bar{1}$ 00] directions provide the atomic structure information of the Ti₃C₂T_x layers. Figure 1h,i clearly show the restacking of Ti₃C₂T_x MXene layers, with each Ti₃C₂T_x MXene layer containing five atomic layers: the two outer atomic layers are Cl atoms, and the three core atomic layers are Ti atoms. This observation matches well with previous results reported for Cl-terminated Ti₃C₂T_x MXenes.^[11,16,17] The observed structure is completely different from the pristine Ti₃AlC₂ MAX phase precursor because no Al atomic layer was observed between the Ti₃C₂ layers, confirming the removal of Al by chemical etching.

Overviews of the X-ray photoelectron spectroscopy (XPS) spectra of the Ti₃AlC₂ precursor (black) and Ti₃C₂T_x MXene (red) are shown in Figure S2. While the Ti, C, and O signals are present for both the Ti₃AlC₂ MAX precursor and Ti₃C₂T_x MXene samples, the Cl signal is only detected for the Ti₃C₂T_x MXene, which confirms the presence of Cl surface groups. Moreover, the Ti–Al bond signal at 73.5 eV and Al signal at 71.5 eV are not visible for the Ti₃C₂T_x MXene (Figure S2b), confirming the removal of the Al layer.^[18,19] The Al–O peak could be caused by a small hydrolysis product of AlCl₃, as reported previously,^[20] or Al₂O₃ impurities from the precursors.^[21] The Ti 2p XPS spectrum of the Ti₃C₂T_x MXene is shown in Figure S3a. The peaks at 454.5 and 456.0 eV are assigned to Ti–C (I) (2p_{3/2}) and Ti–C (II) (2p_{3/2}) bonds, while the peaks at 460.4 and 461.8 eV correspond to Ti–C (I) (2p_{1/2}) and Ti–C (II) (2p_{1/2}) bonds.^[22,23] In addition, the peaks at 458.4, 464.3, 457.9, and 463.6 eV can be associated with Ti–O (2p_{3/2}), Ti–O (2p_{1/2}), Ti–Cl (2p_{3/2}), and Ti–Cl (2p_{1/2}) bonds,^[20,22,24] respectively. The Ti–O and Ti–Cl chemical bonds confirm the presence of –Cl and –O surface groups on the Ti₃C₂T_x MXene. Furthermore, the existence of –O surface groups is verified by the fit C 1s (Figure S3b) and O 1s (Figure S3c) spectra. Additional information on the XPS analysis is shown in the Supporting Information (Figure S3 and Table S2).

In the next step, the synthesis process was scaled by etching large batches (20 and 60 g) of the Ti₃AlC₂ MAX phase. The XRD patterns (Figure 2a) of the Ti₃C₂T_x prepared from 0.5, 20 and 60 g batches exhibited no differences, with the same characteristic peaks located at the same 2θ angles. The SEM images in Figure 2b–d show that the structural morphology of the Ti₃C₂T_x MXene prepared from the large batches was almost identical to that of the MXene from the small batch of 0.5 g, demonstrating the scalability of the MS³ method. This argument is also validated by XPS analysis. These characterizations confirm no distinct structural or chemical state differences between the samples produced in 0.5 g and 20 g batches (Figure S3). Hence, we believe that this MS³ method can be scaled for the industrial production of Ti₃C₂T_x MXenes owing to its simplicity. In addition, the yield rate of Ti₃C₂T_x MXene was calculated. Starting with 20 g of Ti₃AlC₂ MAX, 14.46 g of Ti₃C₂T_x MXene was obtained after washing with APS, giving a yield rate of 72.3%.

In addition to its simplicity and scalability, the MS³ route allows for the preparation of various MXenes, including Ti₂CT_x, Ti₃CNT_x, and Ti₄N₃T_x. Figure 3a–c show that all characteristic peaks of the MAX phases disappeared from the XRD patterns, while the (00l) peaks shifted to lower 2θ angles after etching, indicating the successful synthesis of the corresponding MXenes. Furthermore, SEM images (Figure 3d–f) show multilayered MXenes. Many small particles were observed on the

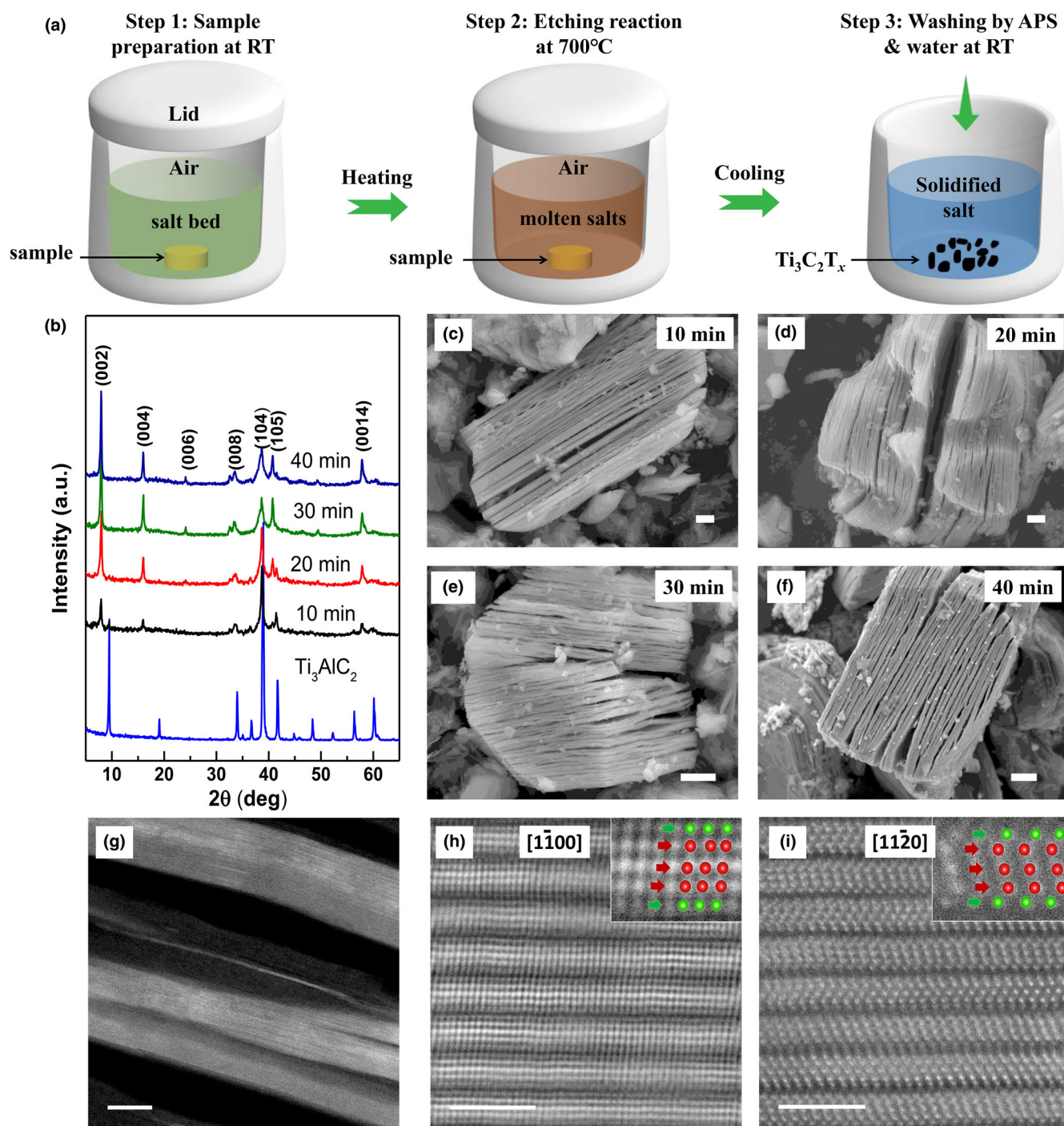


Figure 1. a) Scheme of molten salt-shielded synthesis (MS^3) of $Ti_3C_2T_x$ MXene in air. The sample (pellet) contains NaCl/KCl and Ti_3AlC_2 MAX phase mixture, and the salt bed is NaCl/KCl mixture with a 1:1 mole ratio mixed with $CuCl_2$ etchant. b) XRD patterns of the pristine Ti_3AlC_2 MAX phase and samples after 10–40 min of etching at 700 °C and c–f) corresponding SEM images: c) 10, d) 20, e) 30, and f) 40 min; scale bars are 1 μm . g) TEM image of the $Ti_3C_2T_x$ MXene, scale bar 20 nm. h, i) Atomic-resolution HAADF-STEM images of the $Ti_3C_2T_x$ MXene along the h) $[1\bar{1}00]$ and i) $[11\bar{2}0]$ projections; insets are magnified views of atomic locations.

MXene particle surfaces, particularly on the Ti_2CT_x MXene sample, which could be explained by aluminum oxide, as discussed in the XPS analysis. EDS maps (Figures S4–S6) show the homogeneous distribution of elements, including Ti, Al, C, N, Cl, Cu, and O, and particle-like

aggregation of Al and O, confirming the presence of aluminum oxide particles on the surface of MXenes. The Al and Cu contents are considerably low in the MXenes (Table S1), indicating the removal of Al by chemical etching and the removal of Cu by APS washing. TEM images

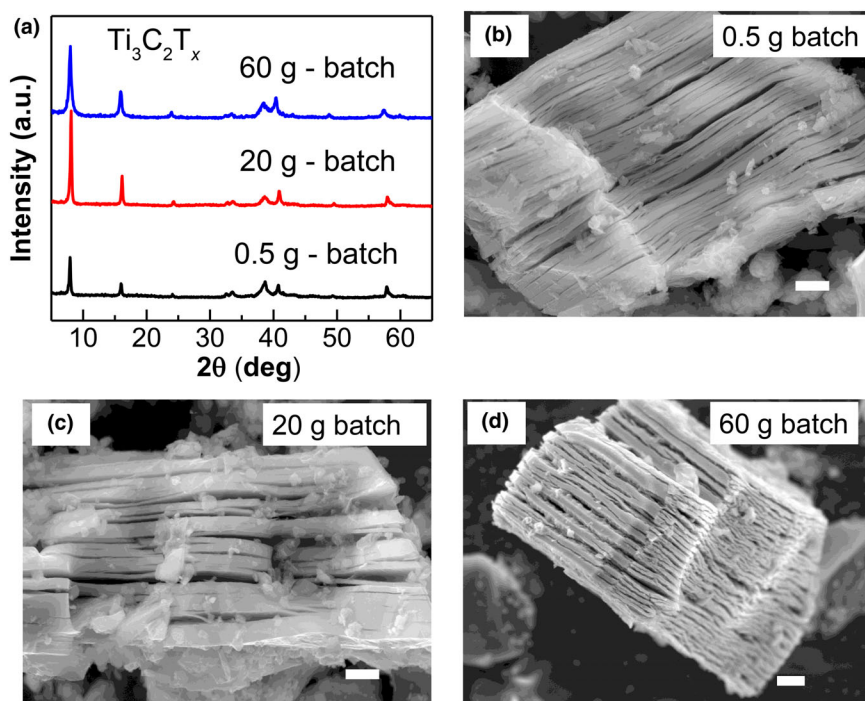


Figure 2. Characterizations of $\text{Ti}_3\text{C}_2\text{T}_x$ MXenes obtained from 0.5, 20 and 60 g batches of Ti_3AlC_2 MAX precursors. a) XRD patterns and b–d) SEM images; scale bars are 1 μm .

(Figure 3g–i) confirm the multilayered structure of the prepared MXenes, in good agreement with previously reported results.^[8,11] In addition, Figures S7–S9 present the XPS spectra of $\text{Ti}_4\text{N}_3\text{T}_x$, Ti_3CNT_x , and Ti_2CT_x , respectively. All XPS spectra confirm the removal of Al in the MAX phases and the successful synthesis of the corresponding MXenes. More information is provided in Tables S3–S5. Note that nitride MXenes are typically difficult to obtain using most MXene synthesis methods. For example, the $\text{Ti}_4\text{N}_3\text{T}_x$ MXene has only been synthesized using molten fluoride salts.^[6,25] Thus, the MS^3 method has proven to be a general method for preparing both carbide and nitride MXenes. The yield rates of the Ti_2CT_x , Ti_3CNT_x , and $\text{Ti}_4\text{N}_3\text{T}_x$ MXenes from the corresponding MAX phases were 65%, 78%, and 70%, respectively.

The electrochemical properties of the MS^3 -MXenes were investigated in half (coin) cells with MXenes as working electrodes and lithium foils as counter and reference electrodes. Cyclic voltammetry (CV) profiles of various MXenes are shown in Figure S10 at scan rates from 0.5 to 20 mV s^{-1} . As shown, $\text{Ti}_4\text{N}_3\text{T}_x$ is considerably less promising as a lithium storage anode because of its lower specific capacity and higher delithiation potential (Figure S10d). In the CV curves of the Ti_2CT_x , Ti_3CNT_x , and $\text{Ti}_3\text{C}_2\text{T}_x$ electrodes (Figure 4a), no noticeable redox peaks were observed, as typically achieved with battery-type materials, and a constant current was obtained in a broad potential range, particularly for the delithiation process; this is similar to the intercalation pseudocapacitive behavior reported for Nb_2O_5 in Li^+ -containing nonaqueous electrolytes.^[26] In addition, the electrochemical signatures agree well with those of a recently reported molten salt prepared MXene (MS^3 -MXene).^[8] Figure 4b presents the galvanostatic charge-discharge curves of the Ti_2CT_x , Ti_3CNT_x , and $\text{Ti}_3\text{C}_2\text{T}_x$ MXenes at 0.1 A g^{-1} . A maximum reversible specific capacity of 280 mAh g^{-1} was delivered with the

Ti_2CT_x MXene electrode, which outperformed the maximum capacity of MS^3 - Ti_2CT_x .^[8] The rate performances of Ti_2CT_x , Ti_3CNT_x , $\text{Ti}_3\text{C}_2\text{T}_x$, and $\text{Ti}_4\text{N}_3\text{T}_x$ at different specific currents were tested (Figure S11) after pre-cycling at a current density of 0.1 A g^{-1} , and the results are summarized in Tables S6–S9. A maximum specific capacity of 295 mAh g^{-1} was achieved with the Ti_2CT_x MXene electrode at 0.05 A g^{-1} . When the discharge rate was increased to 0.1, 0.2, 0.5, 1.0, 2.0, and 5 A g^{-1} , the Ti_2CT_x electrode retained capacities of 280, 260, 230, 200, 165, and 115 mAh g^{-1} , respectively. The $\text{Ti}_3\text{C}_2\text{T}_x$ and Ti_3CNT_x electrodes had lower specific capacities than that of the Ti_2CT_x electrode, and further study is needed to understand the charge storage mechanism. Figure 4c compares the specific capacities of the MXene electrodes prepared in this work (MS^3 -MXene) with those of MXene electrodes obtained by HF etching and Lewis salt etching methods at different C rates. The MS^3 -MXenes achieved a higher capacity and improved power performance for lithium-ion storage compared with those of MS- and HF-prepared MXenes.^[8,27,28] Figure 4d shows the cycling stability of the MXene electrodes at a specific current of 1 A g^{-1} . The cycling capacities remained stable for 1000 cycles, indicating that these MXene electrodes have good cycling properties. These results demonstrate that MS^3 -MXene electrodes possess excellent electrochemical performance for Li-ion storage in nonaqueous electrolytes.

3. Conclusion

We report the MS^3 method for preparing MXenes in the air using low-melting-point eutectic chlorides as a reaction salt bed and Lewis acid salts as etchants. The molten chloride salt bed prevents direct contact between the MAX precursor and air during the high-temperature etching reaction. Several types of MXenes were successfully prepared using the MS^3 method, and its large-scale production capacity was also highlighted. Moreover, the prepared MS^3 -MXenes achieved excellent electrochemical performance for lithium-ion storage. Compared to other MXene synthesis methods, the MS^3 method does not use any hazardous reactants or inert gas protection and allows for the fast synthesis of both carbide and nitride MXenes. It can be easily scaled to etch 60 g of the MAX phases. We believe that the proposed MS^3 -MXene synthesis method is an important advance that will be of great interest to MXene scientific researchers and industry.

4. Experimental Section

MS^3 of MXenes: Details of the raw materials used in this study are given in Table S10, and the synthesis conditions of various MXenes are summarized in Table S11. Consider the synthesis of $\text{Ti}_3\text{C}_2\text{T}_x$ MXenes as an example. First, 0.5 g of Ti_3AlC_2 MAX phase powder and the eutectic salt ($\text{NaCl}:\text{KCl} = 1:1$ stoichiometric

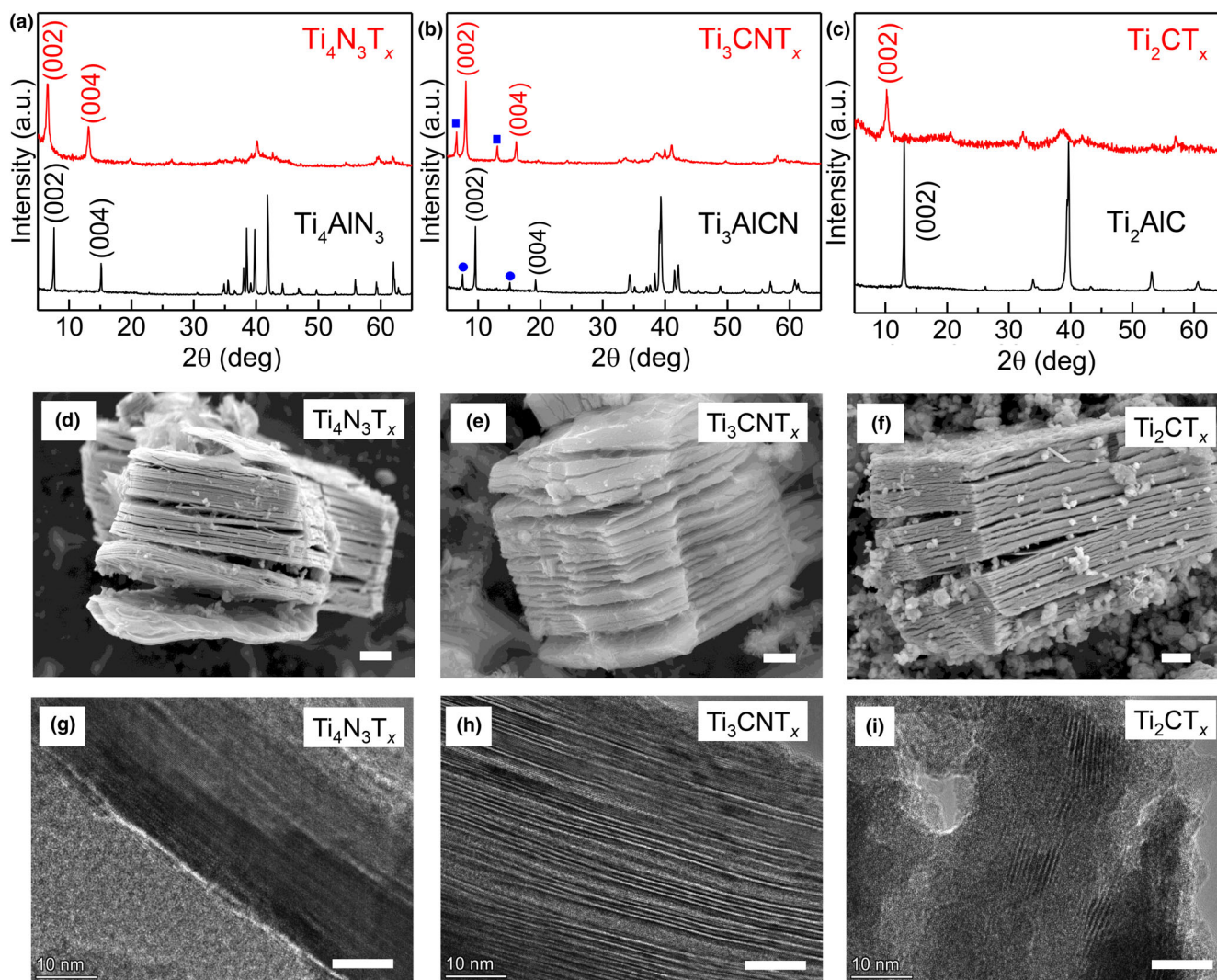


Figure 3. XRD patterns of a) $\text{Ti}_4\text{N}_3\text{T}_x$, b) Ti_3CNT_x , and c) Ti_2CT_x ; the blue circle and square represent the Ti_4AlN_3 impurity and the corresponding $\text{Ti}_4\text{N}_3\text{T}_x$, respectively. d–f) SEM images of $\text{Ti}_4\text{N}_3\text{T}_x$, Ti_3CNT_x , and Ti_2CT_x , respectively; scale bars are 1 μm . g–i) TEM images of $\text{Ti}_4\text{N}_3\text{T}_x$, Ti_3CNT_x , and Ti_2CT_x , respectively; scale bars are 10 nm.

molar ratio) were mixed in a 1:4–6 weight ratio. The mixture was milled for 10 min using a mortar and pestle. The resulting powder was uniaxially pressed in a steel die 20 mm in diameter at a load of 50 kg cm^{-2} to prepare the pellet. Pressing the MAX phase precursors with NaCl/KCl into a pellet is to eliminate the possible oxidation of MAX phases during the heating process. The chloride is added in the pellet to ensure the MAX particles will well disperse in the molten salt at high temperature. The resulting pellet was placed in a cylindrical alumina crucible. Then, a salt mixture containing 8.766 g of NaCl, 11.183 g of KCl, and 2.073 g of CuCl_2 was added to a crucible (30 mL) to cover the pellet after milling for 10 min. The crucible was covered with an alumina lid and then placed in a muffle furnace, which was heated to 700°C at $10^\circ\text{C}/\text{min}$ and held for 10–40 min. After cooling to room temperature, the $\text{Ti}_3\text{C}_2\text{T}_x/\text{Cu}$ mixture was repeatedly washed with deionized water to remove salts. The Cu in the obtained $\text{Ti}_3\text{C}_2\text{T}_x/\text{Cu}$ mixture was removed by washing with 100 mL of 0.5 M APS solution for 1 h at room temperature. The obtained solution was washed more than five times with deionized water, followed by filtration. Finally, the $\text{Ti}_3\text{C}_2\text{T}_x$ MXene powder was dried under vacuum at room temperature for 12 h. Similar etching procedures were followed to etch the larger batches MAX phase and other MAX phases.

Material characterization: The samples were analyzed by XRD (DX-2000) with $\text{Cu K}\alpha$ radiation at 40 kV and 30 mA. The XRD patterns were collected from 5° to

90° with a 0.06° step and a 1 s collection time for each step. The microstructures and chemical compositions (elemental distribution) of the samples were characterized by SEM (JSM-7900F) and EDS (Ultima MAX 65). The chemical states were measured by XPS (AXIS Ultra DLD, Kratos) at a power of 10 kV. TEM and high-resolution TEM images were used to analyze the microstructure. The TEM and STEM samples were prepared using a focused ion beam using a Helios G4 UC with a working voltage of 30 kV. The microstructure and microchemistry of these samples were characterized using a Talos F200X transmission electron microscope equipped with EDS detectors at an acceleration voltage of 200 kV. Atomic structure analysis was conducted using atomic-resolution HAADF-STEM. HAADF-STEM imaging was conducted at 200 kV using a JEOL ARM200F equipped with a cold field emission gun and an ASCOR probe corrector (Guangxi University of Science and Technology, China). HAADF-STEM images were acquired at a convergence semi-angle of 20.9 mrad , resulting in a nominal probe size of 1.28 \AA , and collection angles of 54 to 220 mrad with a camera length of 10 cm.

Electrochemical measurements: All electrochemical measurements were performed using coin cells with electrodes prepared by mixing 80 wt.% MXene powder, 10 wt.% acetylene black, and 10 wt.% PVDF binder. Lithium foil was used as the counter and reference electrodes, 1 M Li-PF_6 in EC/DMC (1/1 by v) was used as the electrolyte, and GFA was used as the separator. The coin cells were assembled in an

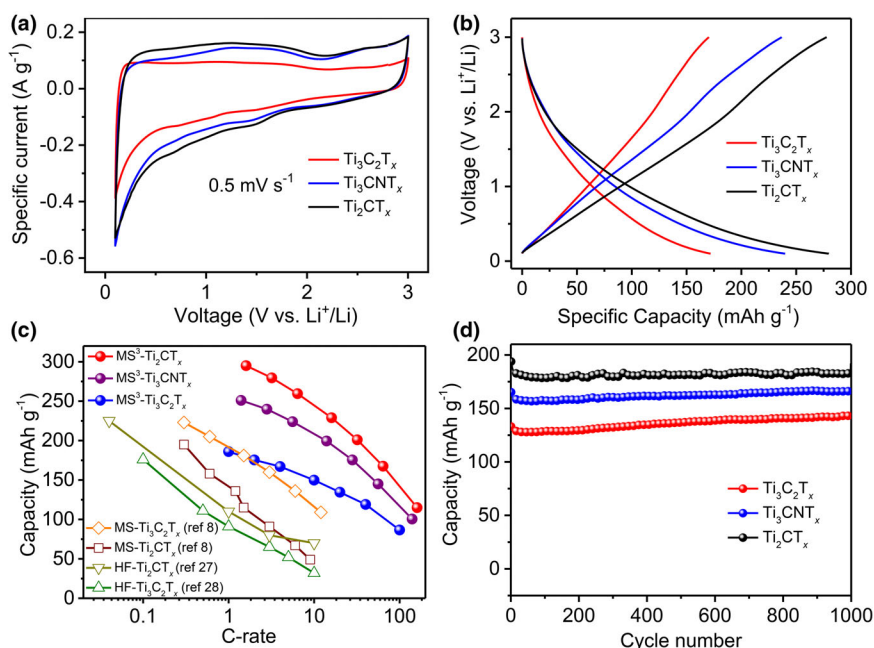


Figure 4. Electrochemical properties of the Ti_2CT_x , Ti_3CNT_x , and $\text{T}_3\text{C}_2\text{T}_x$ MXene electrodes. a) CV curves at 0.5 mV s^{-1} ; b) galvanostatic charge-discharge profiles at 0.1 A g^{-1} ; c) specific capacities of MS^3 -MXenes, MS -MXenes, and HF -MXenes at different C rates; and d) cycling performance at 1 A g^{-1} .

argon-filled glove box with oxygen and water levels of <0.01 ppm. The active material loading of the electrode was approximately 1 mg/cm^2 . All electrochemical tests were conducted using a Biologic VMP3 potentiostat.

Acknowledgements

This study was supported by the National Natural Science Foundation of China (Grant No. 52072252, No. 51902215), and Sichuan Science and Technology Program (No. 2020ZDZX0005), and the Fundamental Research Funds for the Central Universities (YJ201886). P.S., P.-L. T. and H.S. thank the Agence Nationale de la Recherche (Labex STORE-EX) for financial support. Q.H. was supported by the Leading Innovative and Entrepreneur Team Introduction Program of Zhejiang (Grant No. 2019R01003), Ningbo Top-talent Team Program, Ningbo Municipal Bureau of Science and Technology (Grant No. 2018A610005), President's International Fellowship Initiative of CAS (No. 2021DE0002).

Conflict of Interest

The authors declare no conflict of interest.

Supporting Information

Supporting Information is available from the Wiley Online Library or from the author.

Keywords

carbides, lithium-ion storage, molten salt synthesis, MXene, nitrides

Received: November 16, 2021

Revised: November 30, 2021

Published online: November 30, 2021

- [1] Z. Lin, H. Shao, K. Xu, P.-L. Taberna, P. Simon, *Trends in Chem.* **2020**, *2*, 654.
- [2] B. Anasori, M. R. Lukatskaya, Y. Gogotsi, *Nat. Rev. Mater.* **2017**, *2*, Article number: 16098.
- [3] A. VahidMohammadi, J. Rosen, Y. Gogotsi, *Science* **2021**, *372*, eabf1581.
- [4] M. Naguib, M. Kurtoglu, V. Presser, J. Lu, J. Niu, M. Heon, L. Hultman, Y. Gogotsi, M. W. Barsoum, *Adv. Mater.* **2011**, *23*, 4248.
- [5] S.-Y. Pang, Y.-T. Wong, S. Yuan, Y. Liu, M.-K. Tsang, Z. Yang, H. Huang, W.-T. Wong, J. Hao, *J. Am. Chem. Soc.* **2019**, *141*, 9610.
- [6] P. Urbankowski, B. Anasori, T. Makaryan, D. Er, S. Kota, P. L. Walsh, M. Zhao, V. B. Sheno, M. W. Barsoum, Y. Gogotsi, *Nanoscale* **2016**, *8*, 11385.
- [7] T. Li, L. Yao, Q. Liu, J. Gu, R. Luo, J. Li, X. Yan, W. Wang, P. Liu, B. Chen, W. Zhang, W. Abbas, R. Naz, D. Zhang, *Angew. Chem. Int. Ed.* **2018**, *57*, 6115.
- [8] Y. Li, H. Shao, Z. Lin, J. Lu, L. Liu, B. Duployer, P. O. Å. Persson, P. Eklund, L. Hultman, M. Li, K. Chen, X.-H. Zha, S. Du, P. Rozier, Z. Chai, E. Raymundo-Piñero, P.-L. Taberna, P. Simon, Q. Huang, *Nat. Mater.* **2020**, *19*, 894.
- [9] T. Habib, X. Zhao, S. A. Shah, Y. Chen, W. Sun, H. An, J. L. Lutkenhaus, M. Radovic, M. J. Green, *NPJ 2D Mater. Appl.* **2019**, *3*, 8.
- [10] A. Dash, R. Vaßen, O. Guillon, J. Gonzalez-Julian, *Nat. Mater.* **2019**, *18*, 465.
- [11] G. Ma, H. Shao, J. Xu, Y. Liu, Q. Huang, P.-L. Taberna, P. Simon, Z. Lin, *Nat. Commun.* **2021**, *12*, 5085.
- [12] J. Haemers, R. Gusmão, Z. Sofer, *Small Methods* **2020**, *4*, 1900780.
- [13] S. Gupta, Y. Mao, *J. Phys. Chem. C* **2021**, *125*, 6508.
- [14] J. Gonzalez-Julian, *J. Am. Ceram. Soc.* **2021**, *104*, 659.
- [15] M. Shekhirev, C. E. Shuck, A. Sarycheva, Y. Gogotsi, *Prog. Mater. Sci.* **2020**, *120*, 100757.
- [16] J. Lu, I. Persson, H. Lind, J. Palisaitis, M. Li, Y. Li, K. Chen, J. Zhou, S. Du, Z. Chai, Z. Huang, L. Hultman, P. Eklund, J. Rosen, Q. Huang, P. O. Å. Persson, *Nanoscale Adv.* **2019**, *1*, 3680.
- [17] V. Kamyshbayev, A. S. Filatov, H. Hu, X. Rui, F. Lagunas, D. Wang, R. F. Klie, D. V. Talapin, *Science* **2020**, *369*, 979.
- [18] S. Myhra, J. A. A. Crossley, M. W. Barsoum, *J. Phys. Chem. Solids* **2001**, *62*, 811.
- [19] M. W. Barsoum, A. Crossley, S. Myhra, *J. Phys. Chem. Solids* **2002**, *63*, 2063.
- [20] M. Li, J. Lu, K. Luo, Y. Li, K. Chang, K. Chen, J. Zhou, J. Rosen, L. Hultman, P. Eklund, P. O. A. Persson, S. Du, Z. Chai, Z. Huang, Q. Huang, *J. Am. Chem. Soc.* **2019**, *141*, 4730.
- [21] L.-Å. Näslund, P. O. Å. Persson, J. Rosen, *J. Phys. Chem. C* **2020**, *124*, 27732.
- [22] M. Han, X. Yin, H. Wu, Z. Hou, C. Song, X. Li, L. Zhang, L. Cheng, *ACS Appl. Mater. Interfaces* **2016**, *8*, 21011.
- [23] J. Halim, K. M. Cook, M. Naguib, P. Eklund, Y. Gogotsi, J. Rosen, M. W. Barsoum, *Appl. Surf. Sci.* **2016**, *362*, 406.
- [24] C. Mousty-Desbuquoit, J. Riga, J. J. Verbist, *J. Chem. Phys.* **1983**, *79*, 26.
- [25] A. Djire, H. Zhang, J. Liu, E. M. Miller, N. R. Neale, *ACS Appl. Mater. Interfaces* **2019**, *11*, 11812.
- [26] J. Come, V. Augustyn, J. W. Kim, P. Rozier, P.-L. Taberna, P. Gogotsi, J. W. Long, B. Dunn, P. Simon, *J. Electrochem. Soc.* **2014**, *161*, A718.
- [27] M. Naguib, J. Come, B. Dyatkin, V. Presser, P.-L. Taberna, P. Simon, M. W. Barsoum, Y. Gogotsi, *Electrochem. Commun.* **2012**, *16*, 61.
- [28] D. Sun, M. Wang, Z. Li, G. Fan, L.-Z. Fan, A. Zhou, *Electrochem. Commun.* **2014**, *47*, 80.